Journal of Textiles and Polymers
Vol. 11, No. 3, 29-38, June 2023
https://www.itast.ir
DOI: 10.48302/jtp.2024.448732.1284

Experimental and analytical study on tensile strength of short-fiber-reinforced adobe (SFRA)

Mohammad Reza Mirjalili[1], Saeid Fattahi[1], Mohammad Saleh Ahmadi[*1]

[1] Department of Textile Engineering, Yazd University, Yazd, 89195-741, Iran

Article Information

Article history:

Received: 2024-03-15

Accepted: 2024-06-16

***Keywords*:**

Short-fiber reinforced adobe (SFRA), Textile fibers, Tensile strength, Rule of mixtures, Analytical model.

Abstract

The exploration of reinforcing adobe with fibers is pivotal in revolutionizing sustainable construction methods and fortifying the resilience of traditional building materials. This study delves into the impact of incorporating three reinforcement fiber types—glass, polyester, and polypropylene, featuring lengths of 6, 12, and 18mm, and weight percentages of 0.5, 1, and 1.5—on the direct tensile strength of adobe. Additionally, an analytical model based on the modified rule of mixtures was utilized, both with and without porosity consideration, to predict the tensile strength of reinforced adobe. The results indicate that an increase in fiber length and percentage generally augments the tensile strength of samples across all three fiber types, except in cases where excessive elevation of these parameters disrupts proper fiber/mortar adhesion. Notably, samples reinforced with polypropylene fibers exhibited higher tensile strength, with a peak value of 0.69 MPa (using 6mm fibers at 1.5 wt.%), while the lowest value at 0.31 MPa was observed in the sample reinforced with 6mm glass fiber at 0.5 wt.%. The theoretical model provides acceptable predictions for polyester and polypropylene-reinforced samples, with average prediction percentage errors of 16.5% and 13%, respectively. This accuracy is achieved when porosity is considered and samples with excessive fiber lengths and percentages are excluded.

1 INTRODUCTION

Indigenous architecture has the least destructive effect on the ecosystem and environment. The application of indigenous techniques and knowledge, as well as local materials for construction across different geographical areas of the globe, has been ongoing for thousands of years [1,2].

Developing adobe blocks can significantly benefit the environment, particularly in terms of mitigating global warming and climate change, and can also contribute to minimal energy and resource utilization [3]. By 2012, about 30% of the world's population had been living in the oldest and most spacious constructions, i.e. soil-based materials. Such a rate reached 50% in developing countries, most of which lived in rural areas and at least 20% in urban and suburban areas. Roughly 17% of the world's population lived in buildings containing soil-based materials in 2016 [3,4]. Despite the global utilization of soil as a construction material, there are real and significant limitations to its structural use. Their relatively low strength properties compared to concrete foundation blocks and baked bricks have limited their structural use [5].

The historical use of fibers to enhance and modify the behavioral characteristics of soil dates back many years. Hejazi et al. have emphasized the exploration of synthetic short fibers and other applied materials, investigating their role in soil strength and the influence of soil properties, a pursuit that began in the late 1980s [6]. Indeed, the principles of textile engineering have long contributed to enhancing the mechanical properties of soil materials and structures. In the realm of soil and adobe reinforcement, textile fabrics and fibers play a pivotal role, with geotextiles and geogrids typically employed to stabilize loose soil structures [7], while short fibers are commonly integrated into solid matrices, such as adobe, to enhance their mechanical properties and durability. Various methodologies have been employed to address the limitations of adobe architecture. For instance, Sharma et al. [8] reinforced adobe with natural fibers at varying ratios of 0.5%, 1%, 1.5%, and 2%, reporting increased strength with different proportions. Olacia et al. [9] examined the impact of incorporating natural straw fibers and a specific type of sea plant at 0.5%, 1.5%, and 3% weight percentages, along with varying lengths, on the mechanical properties of adobe. Their findings revealed that incorporating straw fibers led to a 69% increase in compressive strength and a 37%

[*] Corresponding Author: ms.ahmadi@yazd.ac.ir

increase in tensile strength compared to the control sample. Moreover, the appropriate quantity and length of sea-plant fibers resulted in approximately 60% and 46% enhancements in compressive and tensile strength, respectively, compared to the control sample. Ige et al. [10] explored the impact of adding 0.25, 0.5, 0.75, and 1 wt% of banana tree fibers on the mechanical, physical, and thermal properties of adobe. Fiber-reinforced specimens exhibited a respective 53% and 33% increase in tensile strength and compressive strength, compared to non-reinforced samples. Furthermore, the fiber-reinforced adobe specimens demonstrated 18% higher thermal resistance than the unreinforced adobe specimens. The use of waste materials in the construction industry has garnered interest from researchers who are actively developing methodical approaches to quantify, optimize, and test the performance of these materials [11]. Bertelsen et al. [12] incorporated recycled polyethylene (R-PE) fibers into adobe bricks at various fractions (1-5% by weight). Utilizing the digital image correlation (DIC) technique, they analyzed mechanical properties and drying shrinkage deformations in the brick specimens. The results indicated that the addition of R-PE fibers led to improved flexural toughness, flexural strength, and compressive strength, while significantly reducing the extent of shrinkage cracking.

On the other hand, several research studies have aimed to predict the tensile properties of short fiber-reinforced composites. Researchers have proposed various models, including analytical, statistical, energy-based, and numerical models, to forecast the mechanical properties of fiber-reinforced soil. Generally, analytical models are preferred for their ability to predict crucial tensile properties of composite materials with shorter computational times and adequate accuracy [13-17].

In a study conducted on the interfacial shear strength between various textile fibers and adobe, it was shown that polyester, polypropylene, and glass fibers have strong adhesion to adobe [18]. The effect of adding glass and polyester fibers on the mechanical properties of reinforced soil has been investigated in several studies [17-25]. It has also been shown that by adding polypropylene fibers the strength and ductility of soil are improved, its swelling-shrinkage is reduced, the chemical and biological degradation problems are overcome, and the frost resistance is improved [26–30].

It is crucial to acknowledge that the majority of previous studies have been confined to the utilization of a single type of fiber. Few studies have ventured into the realm of comparing various fibers under similar conditions to enhance the mechanical properties of soil. Hence, the primary objective of this study is to bridge this gap by systematically comparing the impact of the three important reinforcing fibers, i.e. glass, polyester, and polypropylene, all under identical conditions, on the adobe's tensile properties. Through this research, we aim to offer a comprehensive understanding of the distinct contributions and potential advantages of the three fiber types in strengthening adobe, shedding light on their comparative effectiveness and applicability in practical adobe reinforcement applications. Additionally, the study aims to propose a simplified analytical model for predicting the tensile strength of short fiber-reinforced adobe (SFRA) by taking into account the length and orientation of the fibers.

2 Material and methods

2-1 Fibers

In this study, three types of textile fibers, i.e., glass, polyester, and polypropylene fibers were used as reinforcements. Several fibers of each type were randomly selected and their diameters were measured by a Projectina optical microscope. The tensile strength, strain, and modulus of the fibers were measured according to ASTM D3822 using the EMT3050 tensile testing machine (by Elima Co.). Each fiber type was tested 30 timeks, and the specifications of the fibers are provided in Table 1.

2-2 Soil characterization

The required clay and sand for building the specimen have been extracted from Yazd city mines. Soil granulation has been made by hydrometric method with a standard of ASTM D7928-17 and by a sieve having a standard of ASTM D6913/D6913M-17. The curve is depicted in Fig. 1.

Table 1 Specifications of the fibers.

Fibers	Diameter (mm)	Length (mm)	Tensile strength (MPa)	Strain at Break (%)	Tensile modulus (GPa)	Density (g/cm^3)
Glass	0.039	6, 12, 18	1930	2.6	70	2.6
CV%	21.12	36.1,18.5,21	32.58	18.3	25.8	37.7
Polyester	0.051	6, 12, 18	161	39	3.3	1.38
CV%	36.11	27.3,19,46.4	50.54	34.8	19.9	27.65
Polypropylene	0.046	6, 12, 18	156	50	1.8	0.91
CV%	11.91	14.6,28,31.2	10.29	12.2	22.5	39.2

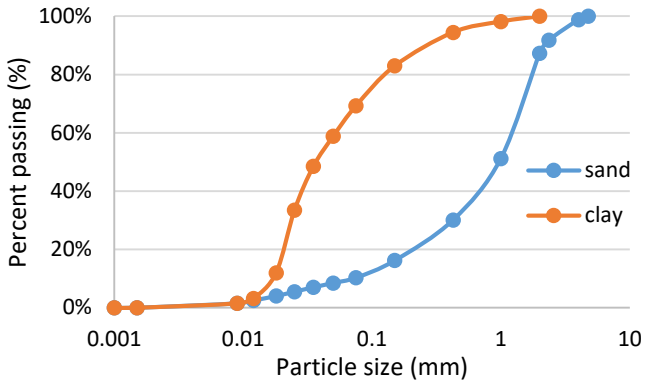

Fig. 1 Clay and sand granulation curves

The physical properties including Atterberg limits and soil plasticity index measured according to ASTM D 4318 and ASTM D 427 are shown in Table 2.

2-3 Mortar preparation

Sand with a diameter of less than 2 mm was employed in the production of the fiber-reinforced adobe mixture, and potable water was used to create the mortar. In order to explore the impact of sand and water on enhancing the tensile strength of fiber-free clay, test specimens were formulated according to the compositions depicted in Fig. 2. The initial number in the code denotes the weight percentage of sand to clay, while the subsequent number indicates the percentage of water weight relative to the combined weights of sand and clay. Following a 28-day period during which the samples were air-dried, they underwent direct tensile testing using the Kardotech universal testing machine at a rate of 0.5 mm/min according to ASTM C307. Although there was no significant difference between the results of the samples 35s28w and 25s35w, observations indicated that more sand and less water resulted in fewer surface and internal cracks. Therefore, the mixing plan 35s28w, which exhibited the highest tensile strength of 0.99 MPa, was selected for this research. Consequently, this specific mix ratio was adopted for the production of all samples in this study. Fig. 3 shows some molded specimens and a specimen undergoing direct tensile testing.

Table 2 The characteristics of the soil

Characteristics	Liquid limit (%)	Plastic index (%)	Plasticity index (%)	Shrinkage limit (%)	Dry unit weight (g/cm^3)
Clay	41	19	22	14	1.75
Sand	36	17	19	12	1.61

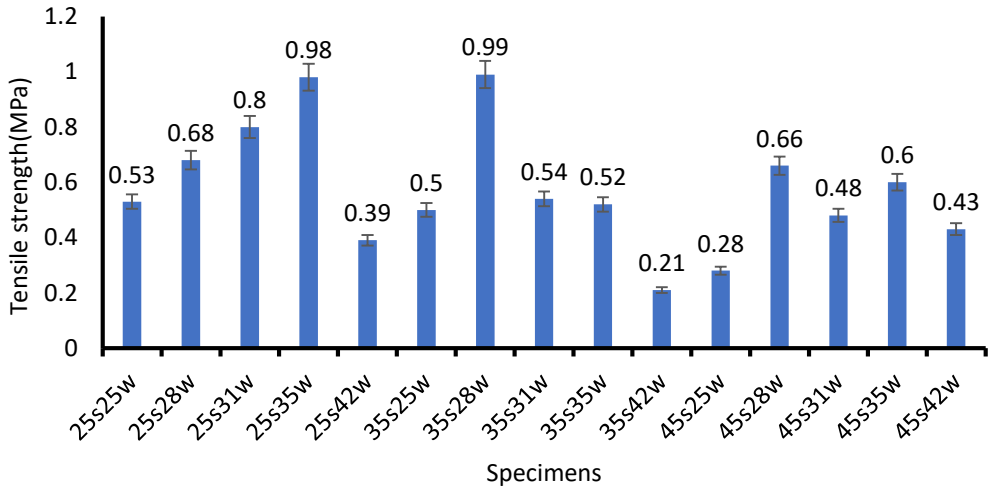

Fig. 2 Tensile strength of adobe samples with different mixing ratios

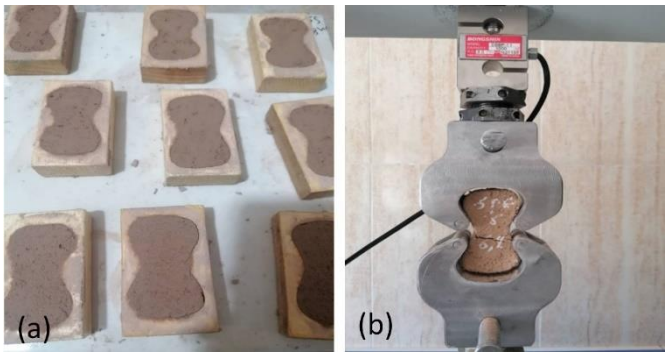

Fig. 3 (a) molded specimens and (b) a specimen under direct tensile testing

The dry clay and sand underwent sieving with a 4 mm2 mesh size to eliminate larger particles before mixing. Subsequently, the sand was combined with clay at a weight ratio of 35%. Fibers, with weight percentages of 0.5, 1, and 1.5, along with water at a weight percentage of 28%, were gradually incorporated into the mixture. Manual blending was used to mix the matrix and fibers, and the resulting mortar was poured into wooden dumbbell-shaped molds conforming to ASTM C307 specifications. To allow for drying, three specimens were produced from each sample and left at room temperature for 28 days. Each sample was labeled with a three-part code, for instance, "G,6,0.5". In this code, the first part denotes the fiber type (G for glass, PE for polyester, and PP for polypropylene), the second part indicates the length of fibers (mm), and the third part signifies the weight percentage of the fibers. The control sample, which included only mortar and no fiber reinforcement, was labeled with the letter C.

2-4 Tensile test

The tensile test of fiber-reinforced adobe samples was performed according to ASTM C307 by the universal testing machine Kardotech with a cross-head speed of 0.5 mm/min. Three samples were tested for each fiber-reinforced adobe mixture.

2-5 Statistical Analysis

The data was subjected to multi-factor analysis of variance (ANOVA) using the SPSS statistical software, and all multiple comparisons were carried out utilizing Duncan's method.

2-6 Prediction of tensile strength

Various analytical models with different levels of accuracy and complexity are utilized for predicting the tensile strength of fibrous composites. Among these, ROM models are popular due to their simplicity and their ability to provide predictions with acceptable accuracy. This category includes the Fukuda-Chou ROM, Cox ROM, Cox-Krenchel ROM, Hirsch ROM, Kelly-Tyson ROM, and Bowyer Bader ROM [31]. While ROM serves as a straightforward model for predicting the tensile strength of continuous fiber composites, the modified rule of mixtures (MROM) has been developed and employed by numerous researchers to address the influence of fiber length and arrangement in composites reinforced with short fibers. Eq. (1) outlines the general form of the MROM, commonly used to forecast the tensile strength of short fiber composites when the fibers are distributed in varying lengths and orientations, assuming a complete surface bond between the fibers and the matrix.

$$\sigma_{cu} = \eta_o \eta_l V_f \sigma_f + V_m \sigma_m \quad (1)$$

where η_o and η_l are, the fiber orientation and fiber length factors, respectively, and the product of η_o and η_l, i.e. $\eta_o\,\eta_l$, is the fiber efficiency factor for the strength of the composite, σ_{cu} and σ_f, denote the ultimate tensile strength of the composite and the fiber, respectively, V_f and V_m are the volume fraction of the fiber and matrix; and σ_m is the matrix stress at the failure of the composite [32].

It should be noted that since in the present study the failure strain of polypropylene and polyester fibers is much higher than the soil failure strain, for these two fibers, the tensile strength of the fibers at the matrix failure strain was considered as σ_f in Eq. (1), because composite failure occurs when the first component fails.

The fiber and the matrix volume fractions can be calculated by knowing the weight fractions and the densities of the components as presented in Eq. (2) and (3):

$$V_f = W_f(\rho_c/\rho_f) \quad (2)$$

$$V_m = W_m(\rho_c/\rho_m) \quad (3)$$

Where W_f and W_m are the weight fractions of the fiber and matrix, respectively and ρ_f, ρ_m, and ρ_c are the densities of fibers, matrix, and composite, respectively.

Concerning the fiber orientation factor, both Kelley and Tyson, along with Cox-Krenchel calculations, suggest that this coefficient can be regarded as 0.2 when considering the 3D random fiber orientation within composite structures [30,31]. Consequently, in this study, the value of 0.2 is adopted to η_o.

Moreover, following the Kelly and Tyson model, given the uniform fiber length (as in this study), the fiber length factor is determined using Eq. (4) and (5):

$$\eta_l = l/2l_c \quad \text{for } l < l_c \quad (4)$$

$$\eta_l = 1 - (\tfrac{l_c}{2l}) \quad \text{for } l \geq l_c \quad (5)$$

Where l represents the length of the fibers and l_c denotes the critical length of the fibers. In other words, l_c signifies the length at which a fiber, if shorter, would not achieve its maximum tensile strength when embedded within the composite and subjected to tensile force. The critical length is calculated according to Eq. (6):

$$l_c = \frac{\sigma_{fu}.d}{2\tau} \quad (6)$$

Where σ_{fu} is the ultimate tensile strength of the fiber (MPa), d is the diameter (mm) of the fiber, and τ is the interfacial shear stress between the fiber and adobe (MPa). The values of τ and l_c, previously calculated in our prior study [18] for the same fiber/adobe systems using the Microbond test, are given in Table 3.

Table 3 Fiber/mortar interfacial shear stress and the critical length of the fibers

Fibers	Interfacial shear stress (MPa)	Critical length (mm)
Glass	0.72 (33.2)	46.6 (19.1)
Polyester	0.64 (39.6)	4.6 (32.1)
Polypropylene	0.80 (11.9)	5.8 (14.2)

* The values in parentheses indicate the coefficient of variation percentage (CV %) of the data.

In order to investigate the effect of including the void volume fraction (porosity) in the theoretical model, this parameter (V_p) was calculated using Eq. (7).

$$V_p = \frac{\rho_{ct} - \rho_{ce}}{\rho_{ct}} \quad (7)$$

where ρ_{ct} and ρ_{ce} are the theoretical and the experimental values of the composite's density [33].

The theoretical composite's density is calculated by Eq. (8).

$$\rho_{ct} = \frac{\rho_f \times \rho_m}{(\rho_m \times W_f) + (\rho_f \times W_m)} \quad (8)$$

To measure the experimental density of the composite, cubic specimens were cut from all the composite samples with precise dimensions, and then the experimental density value was obtained by dividing the weight by the volume of the cubes. Table 4 shows the calculated values for the density of the samples.

Therefore, if the porosity volume fraction is included in the prediction of the strength, the volume fraction of the matrix in Eq. (1) is calculated using Eq. (9):

$$V_m = 1 - V_f - V_p \quad (9)$$

It should be noted that the tensile strength of the matrix (σ_m) used in the calculations was selected as 0.29 MPa, based on the results of the experimental tests on the control sample (refer to Section 3-1).

3 RESULTS AND DISCUSSIONS

3-1 Experimental results

Fig. 4 shows the typical stress-strain curves for the control sample and the samples reinforced with 6 mm length and 1% dosage of the three fibers. As illustrated, the control sample failed at a lower tensile strength and strain compared to the fiber-reinforced samples. This highlights the impact of fiber reinforcement in enhancing the strength and toughness of the composite samples.

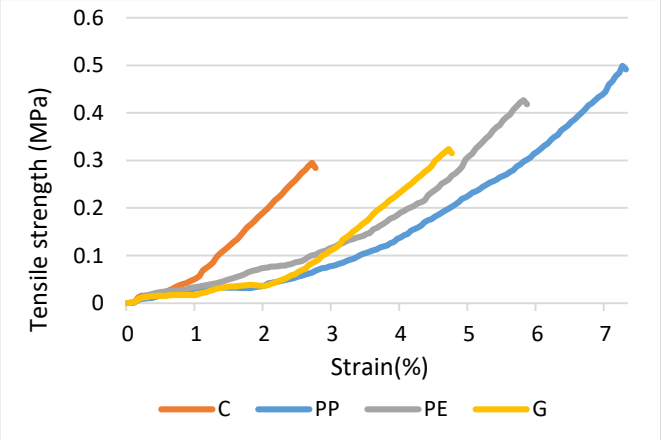

Fig. 4 The stress-strain curve of the adobe sample reinforced with fibers of 6 mm length and 1% dosage

Fig. 5 presents a comparison of the tensile strength among the samples. It is evident that all fiber-reinforced samples exhibit higher tensile strength than the control sample (C).

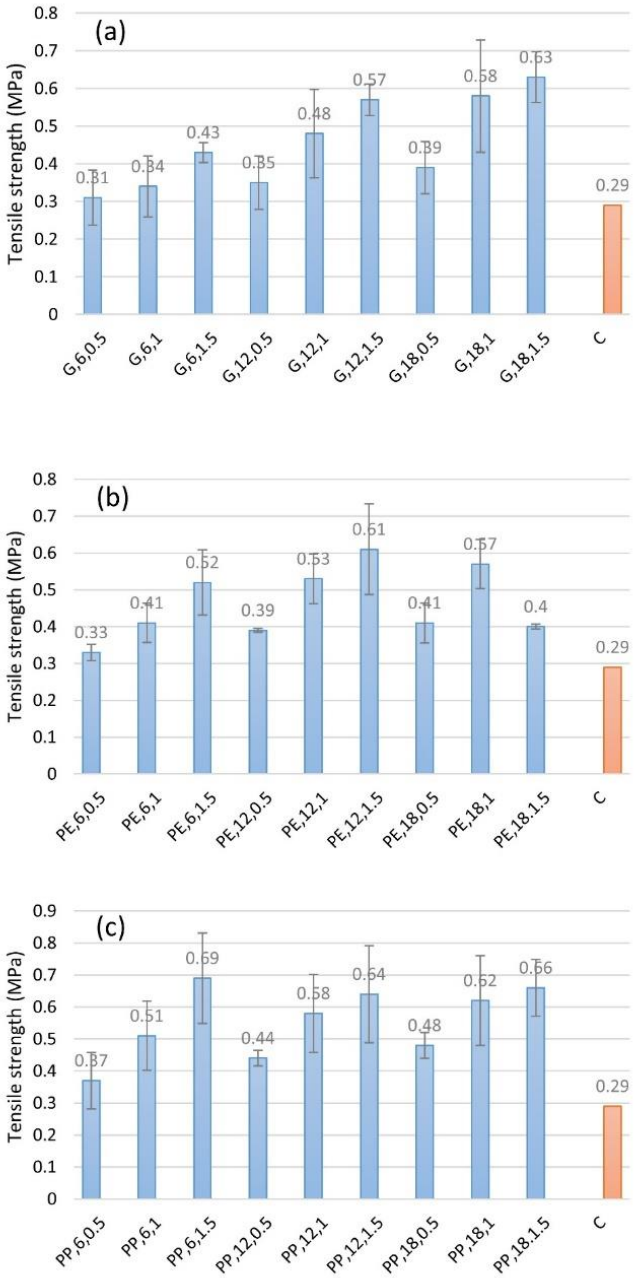

Fig. 5 Tensile strength of the samples reinforced with (a) Glass; (b) Polyester; (c) Polypropylene fibers

Table 4 The density of the composite (adobe reinforced with short fibers) and adobe without fibers

PE 0.5 %(gr/cm^3)	PE1%(gr/cm^3)	PE1.5%(gr/cm^3)	G0.5%(gr/cm^3)	G1%(gr/cm^3)	G1.5%(gr/cm^3)
1.65	1.61	1.53	1.70	1.67	1.59
PP0.5%(gr/cm^3)	**PP1%(gr/cm^3)**	**PP1.5%(gr/cm^3)**	**Adobe(gr/cm^3)**		
1.61	1.58	1.55	1.75		

Furthermore, upon conducting the analysis of variance (Table 5), the significance level is notably smaller than α (0.05), signifying a substantial variance between the mean tensile strength values of clay mortar with short fibers. It shows that the tensile strength is influenced by the parameters of fiber type, fiber length, and fiber dosage.

Table 5 The analysis of variance for the three-factor fixed effects model

Source	Type III Sum of Squares	df	Mean Square	F	Sig.
Fibers	0.177	2	0.088	29.177	.000
Dosage	0.489	2	0.245	80.848	.000
Length	0.126	2	0.063	20.894	.000
Error	0.224	74	0.003		
Total	1.016	80			

The outcomes of Duncan's multiple range test can be found in Table 6, indicating that polypropylene fibers play a more effective role in enhancing the tensile strength of the mortar. This outcome may be attributed to a higher interfacial shear stress between the mortar and polypropylene in comparison to the other two fibers, as previously reported in our study [18].

Table 6 Results of Duncan's Test (a) Fibers, (b) Dosage, and (c) Length

Fibers	N	Subset	
		1	2
G	27	.453	
PE	27	.462	
PP	27		.557
Sig.		.549	1.000

(a)

		Subset		
Dosage	**N**	1	2	3
0.5%	27	.386		
1%	27		.514	
1.5%	27			.572
Sig.		1.000	1.000	1.000

(b)

Length	N	Subset	
		1	2
6mm	27	.436	
12mm	27		.511
18mm	27		.526
Sig.		1.000	.295

(c)

The results from the tensile strength test of the glass fiber-reinforced samples (Fig. 5a) indicate that the specimen reinforced with 0.5 wt% of 6 mm fibers exhibits the lowest tensile strength at 0.31 MPa, while the sample reinforced with 1.5 wt% of 18 mm fibers shows the highest value at 0.63 MPa. An increase in fiber length and volume fraction enhances the tensile strength of glass fiber-reinforced mortar. Upon comparing the tensile strength of samples reinforced with the three fiber types, it becomes apparent that although the tensile strength of glass fiber surpasses that of polyester and polypropylene fibers significantly, the average tensile strength of glass-reinforced samples falls below that of the composite samples reinforced with the other two fibers. This is likely due to two primary reasons. First, the glass fiber features a higher critical length (46 mm) owing to its heightened tensile strength, while the cut length of the fibers in all three cases is notably less than its critical length. Consequently, in the composite samples, the glass fibers never reach their ultimate breaking strength under the applied tensile force but are instead pulled out from the adobe. It is essential to acknowledge that there is a practical maximum limit to the length of the fibers. Excessive increases beyond this limit disrupt proper mixing and significantly raise the viscosity of the mortar during preparation, ultimately diminishing its practical functionality.

In the case of polyester and polypropylene fibers, the cut length of fibers exceeds their critical lengths. As a result, when the adobe reinforced with such fibers is subjected to tensile loading, the fibers reach their maximum breaking strength. Second, glass fibers are known for their brittleness and susceptibility to flexing and abrasion. Consequently, they may incur damage during mixing in the mortar, leading to a reduction in their length and strength. Consequently, glass fibers demonstrate a lower capacity to reinforce adobe than the other two fibers.

When considering the impact of fiber length and dosage, it is apparent that while an increase in both parameters has enhanced the tensile strength of glass fiber-reinforced samples, for the polyester and polypropylene samples at the highest fiber dosage (1.5 wt.%), the tensile strength has at times remained relatively unchanged or even decreased (as observed in the PE,18,1.5 sample) in comparison to lower fiber dosages. The discrepancy in behavior between these two fibers and glass fiber can be attributed to the considerably lower density of polyester and polypropylene fibers in comparison to glass fibers. Consequently, at an equivalent weight fraction, they occupy a larger volume within the mortar than glass fibers. Therefore, surpassing a specific limit for the volume fraction of fibers diminishes the adhesion between the mortar and fibers, thereby reducing the tensile strength of the reinforced mortar.

This trend is also noticeable with the longest fiber length (18 mm) in polyester and polypropylene samples. This phenomenon may be attributed to the increased likelihood of folding, bending, and non-straight placement of fibers within the mortar structure, especially with longer and more flexible fibers such as polyester and polypropylene. This issue subsequently diminishes the tensile strength. Thus, it can be affirmed that there exists a specific threshold for the weight fraction and length of the fibers, as an excessive increase in these two parameters results in a reduction of the tensile strength. Overall, it is evident that the sample containing 1.5% of 6 mm polypropylene fibers exhibits the highest tensile strength among the reinforced samples at 0.69 MPa, while the

lowest value is observed in the sample reinforced with 0.5% of 6 mm glass fibers, yielding 0.31 MPa.

It should be noted that the values obtained for the tensile strength of fiber-reinforced adobe samples in this study are similar to or comparable with those reported in previous studies on similar materials [34-36].

3-2 Comparison of the model and the experimental results

The parameters used in calculating the tensile strength of composite samples and the results of the calculations based on the MROM model of Eq. (1) are given in Table 7. It should be noted that the fiber length factor for glass fibers with lengths less than the critical length was calculated using Eq. (4), while for polyester and polypropylene fibers with lengths greater than the critical length, it was calculated using Eq. (5).

Table 7 The models' parameters and results

Sample	G,6,0.5	G,6,1	G,6,1.5	G,12,0.5	G,12,1	G,12,1.5	G,18,0.5	G,18,1	G,18,1.5
V_f	0.0034	0.0068	0.0102	0.0034	0.0068	0.0102	0.0034	0.0068	0.0102
V_p	0.0286	0.0511	0.0966	0.0286	0.0511	0.0966	0.0286	0.0511	0.0966
V'_m *	0.968	0.9421	0.8932	0.968	0.9421	0.8932	0.968	0.9421	0.8932
V_m	0.9966	0.9932	.9898	0.9966	0.9932	0.9898	0.9966	0.9932	0.9898
σ_f (MPa)	1930	1930	1930	1930	1930	1930	1930	1930	1930
η_l	0.064	0.064	0.064	0.1287	0.1287	0.1287	0.1931	0.1931	0.1931
σ_c (MPa)	0.373	0.4560	0.539	0.4579	0.6258	0.7938	0.5424	0.7949	1.047
CV(%)	(2.35)	(2.39)	(.62)	(2.04)	(2.43)	(.74)	(1.79)	(.56)	(1.06)
σ'_c **(MPa)	0.3647	0.4412	0.511	0.4496	0.611	0.7658	0.5341	0.7801	1.02

Sample	PE,6,0.5	PE,6,1	PE,6,1.5	PE,12,0.5	PE,12,1	PE,12,1.5	PE,18,0.5	PE,18,1	PE,18,1.5
V_f	0.0063	0.0129	0.0189	0.0063	0.0129	0.0189	0.0063	0.0129	0.0189
V_p	0.0571	0.08	0.1207	0.0571	0.08	0.1207	0.0571	0.08	0.1207
V'_m *	0.9366	0.9071	0.8604	0.9366	0.9071	0.8604	0.9366	0.9071	0.8604
V_m	0.9937	0.9871	0.9811	0.9937	0.9871	0.9811	0.9937	0.9871	0.9811
σ_f (MPa)	161	161	161	161	161	161	161	161	161
η_l	0.6167	0.6167	0.6167	0.8083	0.8083	0.8083	0.8722	0.8722	0.8722
σ_c (MPa)	0.4133	0.5424	0.6598	0.4521	0.6220	0.7764	0.4651	0.6485	0.8153
CV(%)	(.67)	(1.3)	(1.69)	(.14)	(1.27)	(2.03)	(1.32)	(1.17)	(.17)
σ'_c **(MPa)	.3967	0.5192	0.6248	0.4359	0.5988	0.7414	0.4486	0.6254	0.7803

Sample	PP,6,0.5	PP,6,1	PP,6,1.5	PP,12,0.5	PP,12,1	PP,12,1.5	PP,18,0.5	PP,18,1	PP,18,1.5
V_f	0.0096	0.0190	0.0285	0.0096	0.0190	0.0285	0.0096	0.0190	0.0285
V_p	0.0747	0.0867	0.1041	0.0747	0.0867	0.1041	0.0747	0.0867	0.1041
V'_m *	0.9157	0.8943	0.8674	0.9157	0.8943	0.8674	0.9157	0.8943	0.8674
V_m	0.9904	0.9810	0.9715	0.9904	0.9810	0.9715	0.9904	0.9810	0.9715
σ_f (MPa)	156	156	156	156	156	156	156	156	156
η_l	0.5167	0.5167	0.5167	0.7583	0.7583	0.7583	0.8389	0.8389	0.8389
σ_c (MPa)	0.4419	0.5908	0.7412	0.5143	0.7340	0.9560	0.5385	0.7818	1.03
CV(%)	(2.38)	(2.1)	(2.05)	(.56)	(2.08)	(2.35)	(.85)	(2.27)	(1.34)
σ'_c **(MPa)	0.4203	0.5657	0.7110	0.4927	0.7089	0.9258	0.5168	0.7566	0.9975

*V'_m : Volume fraction of matrix by considering porosity

**σ'_c: Strength of the composite by considering porosity

The percentage error of prediction of the composite strength values was calculated from the model results and experimental results using Eq. (10):

$$Err(\%) = \frac{predicted\ value - experimental\ value}{predicted\ value} \times 100 \quad (10)$$

Fig. 6 shows the percentage error of prediction. In general, it can be seen that the model considering the porosity, has closer results to the experimental ones. On average, the values of the tensile strength of the composite when the porosity is considered, are 3.68% lower than the case without taking into account the porosity.

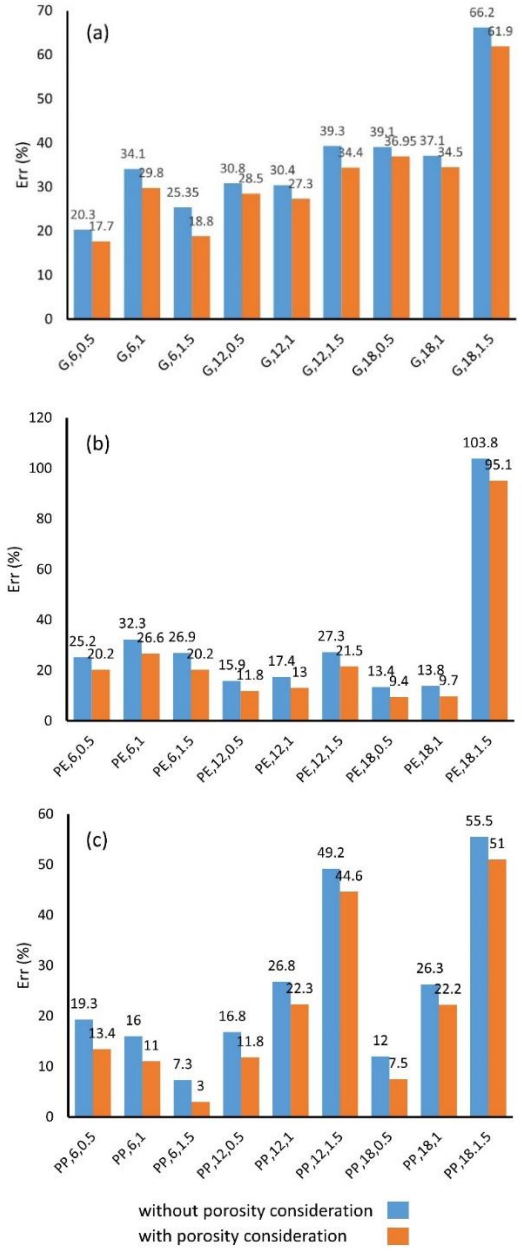

Fig. 6 The percentage error of prediction of tensile strength

As depicted in Fig. 6, the highest prediction errors, both when considering and not considering porosity, are observed for all three types of fibers in samples reinforced with the highest fiber dosage (1.5 wt.%) and longest fiber length (18 mm). This illustrates that with long fibers and high weight percentages, the lack of proper adhesion between fibers and mortar, as well as the increased likelihood of non-linear fiber placement, results in a substantial disparity between predicted and experimental results. The model assumes complete bonding between the fibers and the matrix, along with straight fiber positioning, which contributes to this significant difference. Furthermore, significant errors are also noted for the polypropylene fibers in the sample reinforced with 1.5 wt.% of 12 mm. As previously mentioned, this issue arises from the low density of this fiber, causing it to occupy a larger volume at the same weight, consequently failing to establish proper adhesion with the matrix.

Therefore, excluding cases resulting from excessive fiber weight fractions and lengths, the average prediction error for glass, polyester, and polypropylene-reinforced samples, with porosity considered, would be approximately 28.5%, 16.5%, and 13%, respectively. The higher percentage error for glass fiber-reinforced adobe can be rationalized by the likelihood of fiber damage during mortar preparation, given the brittle nature of this fiber as previously noted. Additionally, the lower error percentage in polypropylene fiber-reinforced adobe may be attributed to the superior adhesion of this fiber to mortar, as indicated in our previous study [18]. Generally, the percentage error values for the samples reinforced with polyester and polypropylene fibers are deemed acceptable for predicting tensile strength within a simple analytical model.

4 CONCLUSIONS

In this study, we examined the impact of incorporating three commonly used fibers—glass, polyester, and polypropylene, each with varying lengths and weight percentages—on the direct tensile strength of fiber-reinforced adobe through experimental investigation. Additionally, we employed an analytical model based on the modified rule of mixtures to predict the tensile strength of the composite samples. Our findings revealed that augmenting the length and weight percentage of fibers (up to a certain extent) enhances the tensile strength of composite samples. However, an excessive increase in these parameters can diminish the tensile strength of the composites due to reduced adhesion between the fibers and the mortar.

Furthermore, samples reinforced with polypropylene fibers exhibited higher average tensile strength values than the other two fibers owing to their superior surface adhesion to clay mortar. Upon comparison of the experimental and predicted results, our analysis demonstrated that when the model accounted for porosity, the predicted results aligned more closely with the experimental findings, averaging 3.68% lower than the predicted results without porosity consideration. By excluding cases where high fiber weight percentages and lengths impede the proper bond between the fibers and the mortar, the prediction percentage error (with porosity considered) for samples reinforced with glass, polyester, and polypropylene fibers were calculated at 28.5%, 16.5%, and 13%, respectively.

REFERENCES

[1] Q. B. Bui, J. C. Morel, B. V. Venkatarama Reddy, and W. Ghayad, "Durability of rammed earth walls exposed for 20 years to natural weathering," *Build. Environ.*, vol. 44, no. 5, pp. 912–919, May 2009, doi: 10.1016/j.buildenv.2008.07.001.

[2] J. . Morel, A. Mesbah, M. Oggero, and P. Walker, "Building houses with local materials: means to drastically reduce the environmental impact of construction," *Build. Environ.*, vol. 36, no. 10, pp. 1119–1126, Dec. 2001, doi: 10.1016/S0360-1323(00)00054-8.

[3] S. Ramakrishnan, S. Loganayagan, G. Kowshika, C. Ramprakash, and M. Aruneshwaran, "Adobe blocks reinforced with natural fibres: A review," *Mater. Today Proc.*, vol. 45, pp. 6493–6499, 2021, doi: 10.1016/j.matpr.2020.11.377.

[4] M. R. A. R. Correia, *Conservation in earthen heritage assessment and significance of failure, criteria, conservation theory, and strategies*. Cambridge Scholars Publishing, 2016.

[5] D. Silveira, H. Varum, A. Costa, T. Martins, H. Pereira, and J. Almeida, "Mechanical properties of adobe bricks in ancient constructions," *Constr. Build. Mater.*, vol. 28, no. 1, pp. 36–44, Mar. 2012, doi: 10.1016/j.conbuildmat.2011.08.046.

[6] S. M. Hejazi, M. Sheikhzadeh, S. M. Abtahi, and A. Zadhoush, "A simple review of soil reinforcement by using natural and synthetic fibers," *Constr. Build. Mater.*, vol. 30, pp. 100–116, May 2012, doi: 10.1016/j.conbuildmat.2011.11.045.

[7] M. S. Ahmadi, and P. Nikbakht Moghadam, "Effect of geogrid aperture size and soil particle size on geogrid-soil interaction under pull-out loading,". *J. Text. Polym.*, vol. 5, no. 1, pp. 25-30.

[8] V. Sharma, H. K. Vinayak, and B. M. Marwaha, "Enhancing sustainability of rural adobe houses of hills by addition of vernacular fiber reinforcement," *Int. J. Sustain. Built Environ.*, vol. 4, no. 2, pp. 348–358, Dec. 2015, doi: 10.1016/j.ijsbe.2015.07.002.

[9] E. Olacia, A. L. Pisello, V. Chiodo, S. Maisano, A. Frazzica, and L. F. Cabeza, "Sustainable adobe bricks with seagrass fibres. Mechanical and thermal properties characterization," *Constr. Build. Mater.*, vol. 239, p. 117669, Apr. 2020, doi: 10.1016/j.conbuildmat.2019.117669.

[10] O. Ige and H. Danso, "Physico-mechanical and thermal gravimetric analysis of adobe masonry units reinforced with plantain pseudo-stem fibres for sustainable construction," *Constr. Build. Mater.*, vol. 273, p. 121686, Mar. 2021, doi: 10.1016/j.conbuildmat.2020.121686.

[11] M. M. Salih, A. I. Osofero, and M. S. Imbabi, "Critical review of recent development in fiber reinforced adobe bricks for sustainable construction," *Front. Struct. Civ. Eng.*, vol. 14, no. 4, pp. 839–854, Aug. 2020, doi: 10.1007/s11709-020-0630-7.

[12] I. M. G. Bertelsen, L. J. Belmonte, G. Fischer, and L. M. Ottosen, "Influence of synthetic waste fibres on drying shrinkage cracking and mechanical properties of adobe materials," *Constr. Build. Mater.*, vol. 286, p. 122738, Jun. 2021, doi: 10.1016/j.conbuildmat.2021.122738.

[13] G. L. Sivakumar Babu, A. K. Vasudevan, and S. Haldar, "Numerical simulation of fiber-reinforced sand behavior," *Geotext. Geomembranes*, vol. 26, no. 2, pp. 181–188, Apr. 2008, doi: 10.1016/j.geotexmem.2007.06.004.

[14] D. H. Gray and H. Ohashi, "Mechanics of Fiber Reinforcement in Sand," *J. Geotech. Eng.*, vol. 109, no. 3, pp. 335–353, Mar. 1983, doi: 10.1061/(ASCE)0733-9410(1983)109:3(335).

[15] M. H. Maher and D. H. Gray, "Static Response of Sands Reinforced with Randomly Distributed Fibers," *J. Geotech. Eng.*, vol. 116, no. 11, pp. 1661–1677, Nov. 1990, doi: 10.1061/(ASCE)0733-9410(1990)116:11(1661).

[16] R. L. Michalowski and A. Zhao, "Failure of Fiber-Reinforced Granular Soils," *J. Geotech. Eng.*, vol. 122, no. 3, pp. 226–234, Mar. 1996, doi: 10.1061/(ASCE)0733-9410(1996)122:3(226).

[17] G. Ranjan, R. M. Vasan, and H. D. Charan, "Probabilistic Analysis of Randomly Distributed Fiber-Reinforced Soil," *J. Geotech. Eng.*, vol. 122, no. 6, pp. 419–426, Jun. 1996, doi: 10.1061/(ASCE)0733-9410(1996)122:6(419).

[18] M. R. Mirjalili, S. Fattahi, and M. S. Ahmadi, "Interfacial Adhesion between Textile Fibers and Clay Mortar," *J. Mater. Civ. Eng.*, vol. 35, no. 2, Feb. 2023, doi: 10.1061/(ASCE)MT.1943-5533.0004547.

[19] T. O. Al-Refeai, "Behavior of granular soils reinforced with discrete randomly oriented inclusions," *Geotext. Geomembranes*, vol. 10, no. 4, pp. 319–333, Jan. 1991, doi: 10.1016/0266-1144(91)90009-L.

[20] N. C. Consoli, J. P. Montardo, P. D. M. Prietto, and G. S. Pasa, "Engineering Behavior of a Sand Reinforced with Plastic Waste," *J. Geotech. Geoenvironmental Eng.*, vol. 128, no. 6, pp. 462–472, Jun. 2002, doi: 10.1061/(ASCE)1090-0241(2002)128:6(462).

[21] N. C. Consoli, M. D. T. Casagrande, P. D. M. Prietto, and A. Thomé, "Plate Load Test on Fiber-Reinforced Soil," *J. Geotech. Geoenvironmental Eng.*, vol. 129, no. 10, pp. 951–955, Oct. 2003, doi: 10.1061/(ASCE)1090-0241(2003)129:10(951).

[22] S. R. Kaniraj and V. G. Havanagi, "Behavior of Cement-Stabilized Fiber-Reinforced Fly Ash-Soil Mixtures," *J. Geotech. Geoenvironmental Eng.*, vol. 127, no. 7, pp. 574–584, Jul. 2001, doi:

10.1061/(ASCE)1090-0241(2001)127:7(574).

[23] A. Kumar, B. S. Walia, and A. Bajaj, "Influence of Fly Ash, Lime, and Polyester Fibers on Compaction and Strength Properties of Expansive Soil," *J. Mater. Civ. Eng.*, vol. 19, no. 3, pp. 242–248, Mar. 2007, doi: 10.1061/(ASCE)0899-1561(2007)19:3(242).

[24] A. Kumar, B. S. Walia, and J. Mohan, "Compressive strength of fiber reinforced highly compressible clay," *Constr. Build. Mater.*, vol. 20, no. 10, pp. 1063–1068, Dec. 2006, doi: 10.1016/j.conbuildmat.2005.02.027.

[25] M. H. Maher and Y. C. Ho, "Mechanical Properties of Kaolinite/Fiber Soil Composite," *J. Geotech. Eng.*, vol. 120, no. 8, pp. 1381–1393, Aug. 1994, doi: 10.1061/(ASCE)0733-9410(1994)120:8(1381).

[26] A. Diambra, E. Ibraim, D. Muir Wood, and A. R. Russell, "Fibre reinforced sands: Experiments and modelling," *Geotext. Geomembranes*, vol. 28, no. 3, pp. 238–250, Jun. 2010, doi: 10.1016/j.geotexmem.2009.09.010.

[27] N. C. Consoli, M. A. Vendruscolo, A. Fonini, and F. D. Rosa, "Fiber reinforcement effects on sand considering a wide cementation range," *Geotext. Geomembranes*, vol. 27, no. 3, pp. 196–203, Jun. 2009, doi: 10.1016/j.geotexmem.2008.11.005.

[28] K. Punthutaecha, A. J. Puppala, S. K. Vanapalli, and H. Inyang, "Volume Change Behaviors of Expansive Soils Stabilized with Recycled Ashes and Fibers," *J. Mater. Civ. Eng.*, vol. 18, no. 2, pp. 295–306, Apr. 2006, doi: 10.1061/(ASCE)0899-1561(2006)18:2(295).

[29] A. J. Puppala and C. Musenda, "Effects of Fiber Reinforcement on Strength and Volume Change in Expansive Soils," *Transp. Res. Rec. J. Transp. Res. Board*, vol. 1736, no. 1, pp. 134–140, Jan. 2000, doi: 10.3141/1736-17.

[30] C. Tang, B. Shi, W. Gao, F. Chen, and Y. Cai, "Strength and mechanical behavior of short polypropylene fiber reinforced and cement stabilized. clayey soil," *Geotext. Geomembranes*, vol. 25, no. 3, pp. 194–202, Jun. 2007, doi: 10.1016/j.geotexmem.2006.11.002.

[31] M. W. Tham *et al.*, "Tensile properties prediction of natural fibre composites using rule of mixtures: A review," *J. Reinf. Plast. Compos.*, vol. 38, no. 5, pp. 211–248, 2019, doi: 10.1177/0731684418813650.

[32] S. Fu, "Effects of fiber length and fiber orientation distributions on the tensile strength of short-fiber-reinforced polymers," *Compos. Sci. Technol.*, vol. 56, no. 10, pp. 1179–1190, 1996, doi: 10.1016/S0266-3538(96)00072-3.

[33] A. C. N. Singleton, C. A. Baillie, P. W. R. Beaumont, and T. Peijs, "On the mechanical properties, deformation and fracture of a natural fibre/recycled polymer composite," *Compos. Part B Eng.*, vol. 34, no. 6, pp. 519–526, Sep. 2003, doi: 10.1016/S1359-8368(03)00042-8.

[34] Ş. Yetgin, Ö. ÇAVDAR, and A. Çavdar, "The effects of the fiber contents on the mechanic properties of the adobes," *Constr. Build. Mater.*, vol. 22, no. 3, pp. 222–227, Mar. 2008, doi: 10.1016/j.conbuildmat.2006.08.022.

[35] H. Mohammadi, A. Eslami, and R. Morshed, "Amirkabir Journal of Civil Engineering Experimental evaluation into improving the mechanical properties of adobe using palm fibers," *Civ. Eng*, vol. 54, no. 6, pp. 465–468, 2022, doi: 10.22060/ceej.2021.19652.7222.

[36] R. Illampas, V. G. Loizou, and I. Ioannou, "Effect of Straw Fiber Reinforcement on the Mechanical Properties of Adobe Bricks," in *Poromechanics VI*, Jul. 2017, pp. 1331–1338, doi: 10.1061/9780784480779.165.